World Academy of Science, Engineering and Technology
International Journal of Materials and Metallurgical Engineering
Vol:11, No:2, 2017

NaCl Erosion-Corrosion of Mild Steel under Submerged Impingement Jet

M. Sadique, S. Ainane, Y. F. Yap, P. Rostron, E. Al Hajri

***Abstract*—**The presence of sand in production lines in the oil and gas industries causes material degradation due to erosion-corrosion. The material degradation caused by erosion-corrosion in pipelines can result in a high cost of monitoring and maintenance and in major accidents. The process of erosion-corrosion consists of erosion, corrosion, and their interactions. Investigating and understanding how the erosion-corrosion process affects the degradation process in certain materials will allow for a reduction in economic loss and help prevent accidents. In this study, material loss due to erosion-corrosion of mild steel under impingement of sand-laden water at 90˚ impingement angle is investigated using a submerged impingement jet (SIJ) test. In particular, effects of jet velocity and sand loading on TWL due to erosion-corrosion, weight loss due to pure erosion and erosion-corrosion interactions, at a temperature of 29-33 °C in sea water environment (3.5% NaCl), are analyzed. The results show that the velocity and sand loading have a great influence on the removal of materials, and erosion is more dominant under all conditions studied. Changes in the surface characteristics of the specimen after impingement test are also discussed.

***Keywords*—**Erosion-corrosion, flow velocity, jet impingement, sand loading.

I. Introduction

EROSION-corrosion causes material degradation in pipelines, pumps, heat exchanger tubes, propellers, impellers, valves, and other fluid handling equipment [1]. Erosion-corrosion is considered as a major challenge in the oil and gas and chemical industries [2]. It is ranked as the fifth most critical degradation mechanism in offshore and chemical industries [3].

Erosion-corrosion in aqueous slurries is dominated by two mechanisms: mechanical erosion and chemical corrosion [4]. In an erosion-corrosion process, the erosion is caused by the mechanical impact of solid particles present in the flow, while corrosion is caused by the electrochemical reaction that takes place on the metal surface when it is exposed to corrosive liquids. The erosion-corrosion process also involves the interaction between erosion and corrosion. These interactions are often referred to as 'synergistic' and 'additive' effects. "The term synergistic is referred to as the process in which the corrosion enhances erosion and the additive effect is referred to as the process in which erosion enhances corrosion" [4]. The behavior of erosion-corrosion is defined by different regimes: corrosion-dominated, erosion-dominated, or erosion-corrosion dominated depending on the material type and the working environments [5].

The mechanism of erosion-corrosion has been widely investigated using different methods in different environments for different materials, and the most common of these methods is the SIJ apparatus [1], [3], [6]-[10]. Hu and Neville [6] studied the effect of velocity, sand loading and fluid temperature on erosion-corrosion of steel (API X65) in a CO_2 environment. Hu and Neville investigated synergistic and additive effect separately. Meng et al. [1] applied a full factorial design method to study the contribution of each processes involving erosion-corrosion and to understand the conditions under which maximum weight loss occurs. Neville et al. [3] conducted a comparative study to analyze the contribution of each process at different temperatures on two different materials. Souza and Neville [10] estimated the percentage contribution of each process to the total weight loss (TWL). Neville and Hodgkiess [11] and Neville et al. [12] considered the contributions of static corrosion and erosion enhanced corrosion together as total corrosion on three different materials. Hu and Neville [4], [6], [8] analyzed the changes in the surface roughness after erosion-corrosion tests. Naz et al. [13] focused on the changes in surface profile and composition after impingement tests. However, the processes involving the erosion-corrosion mechanism on mild steel in sea water environment is still poorly understood, especially the interaction between erosion and corrosion. Hence, the purpose of this work is to investigate the effect of velocity and sand concentration on the erosion-corrosion on mild steel in sea water. A submerged impingement apparatus was developed with the aim to investigate:

1. The velocity effect and sand loading effect on erosion-corrosion and pure erosion.
2. The behavior of erosion-corrosion interaction with the different flow velocity and sand loading.
3. The changes on surface of sample materials at different conditions.

II. Methodology

A. Materials

The samples used in this study were made of mild steel, with an area of 4 cm^2. The samples were polished to mirror finish (oxide polishing) using Tegrapol-21 polishing machine

Muhammed Sadique is with The Petroleum Institute, Abu Dhabi, United Arab Emirates (phone: 971561912105; e-mail: mup@pi.ac.ae).

Sami Ainane was with the Maryland University, College Park, MD 20742, USA. He is now with the Department of Mechanical Engineering, The Petroleum Institute, Abu Dhabi, United Arab Emirates (phone: 971026075983; e-mail: sainane@pi.ac.ae).

YAP Yit Fatt is with the Department of Mechanical Engineering, The Petroleum Institute, Abu Dhabi, United Arab Emirates (phone: 971026075175; e-mail: yfatt@pi.ac.ae).

Paul Rostron is with the Department of Chemistry, The Petroleum Institute, Abu Dhabi, United Arab Emirates (phone: 971026075217; e-mail: prostron@pi.ac.ae).

and a micro-cloth containing a suspension of oil soluble aluminum oxide. The samples were cleaned with acetone and distilled water and dried. Table I shows the chemical composition of the parent metal, obtained using X-ray fluorescence. Silica sand with an average size of 125-250 µm was used as the erodent particles, SEM image of silica sand used is shown in Fig. 1.

TABLE I
CHEMICAL COMPOSITION OF MILD STEEL USED IN THIS STUDY

Element	Weight percentage
Aluminum	0.014
Silicon	0.185
Phosphorous	0.009
Sulphur	0.012
Chromium	0.064
Manganese	0.438
Iron	98.887
Cobalt	0.182
Nickel	0.043
Copper	0.086
Zinc	0.013
Molybdenum	0.011
Carbon	0.057

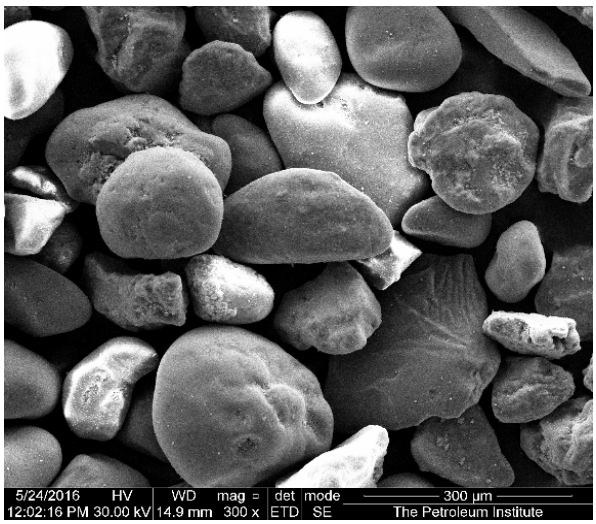

Fig. 1 SEM image of 125-250 µm silica sand particles

B. SIJ Rig

Erosion-corrosion tests were carried using a SIJ apparatus as shown in Fig. 2. The centrifugal pump in the recirculating rig enables uniform mixing of sand particles with the water which is delivered through the nozzle impinging on the surface of the sample at an angle 90˚. The nozzle has an exit diameter of 4 mm and it is fixed at a distance of 5 mm from the sample. A cooling coil was used to compensate for water temperature rises due to friction in the pump.

C. Test Conditions

Pure erosion tests were conducted in tap water containing 150 ppm sodium sulfite, which acts as an oxygen scavenger. Salt water containing 3.5% NaCl was used for the erosion-corrosion tests.

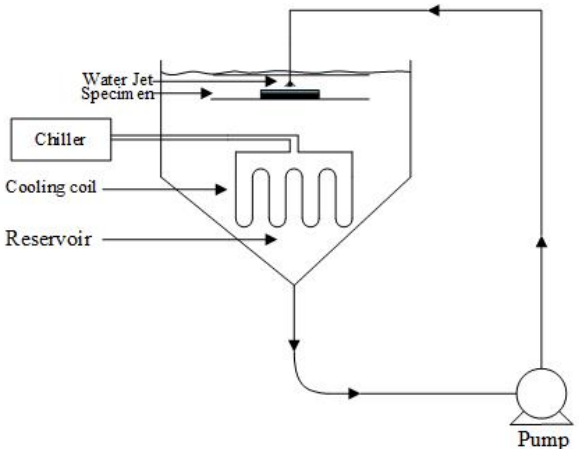

(a) Schematic of experimental rig

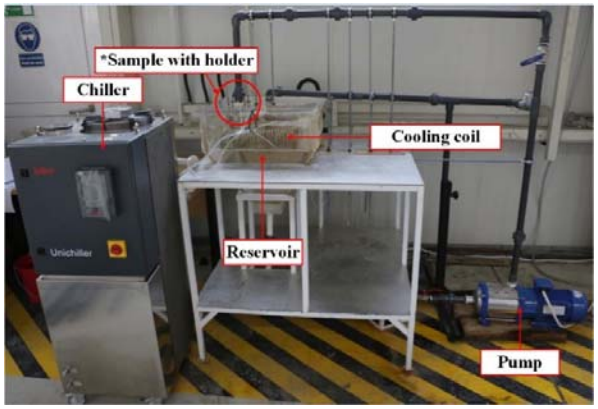

(b) Photograph of the experimental rig

Fig. 2 Recirculating rig

The linear polarization method was used to measure static corrosion as it is considered more accurate than the Tafel extrapolation method [14], [15]. The linear polarization resistance (R_P) was measured using an electrochemical cell (potentiostat) with three electrodes, graphite as a counter electrode, silver as a reference electrode and the sample as the working electrode. The potential of the working electrode was scanned from − 20 mV to + 20 mV at a rate of 25 mV/s. The corrosion current density (i_{corr}) was calculated using (1) where the Tafel constants β_a and β_c are assumed to be 30 mV/decade as erosion-corrosion involves active dissolution of material under solid-liquid impingement [6].

A digital balance with a precision of ±0.1 mg was used to measure the weight loss due to pure erosion and the erosion-corrosion TWL.

The experiments were conducted for jet velocities of 10, 13, 16, and 20 m/s and sand loadings of 300, 400, 500, and 600 mg/l. The water temperature was kept in the range of 29-33 °C. All the experiments were repeated three times.

$$i_{corr} = \frac{\beta_a \beta_c}{2.303 R_P(\beta_a + \beta_c)} \quad (1)$$

III. Results and Discussion

A. Observations from Erosion-Corrosion Measurements

The effect of time on TWL due to erosion-corrosion was investigated to better understand the rate of material degradation with time. Fig. 3 clearly shows that the TWL of the specimen increases linearly with time, at least for the first four hours of impingement. The same trend was obtained by Hu and Neville [6] when investigating the effect of erosion-corrosion on API X65. Fig. 4 shows the SEM images of the center of the specimen (diameter (ø) < 1 mm), after impingements for one and four hours. The images show signs of plastic deformation. The SEM images also show the formation of discrete isolated pits and ploughing tracks after one hour of impingement (Fig. 4 (a)). Fig. 4 (b) shows that after four hours of impingement, the pits become larger holes and show thick elongated tracks. This is consistent with observations made by Neville and Hu [8] and by Shrestha and Hodgkgies [16].

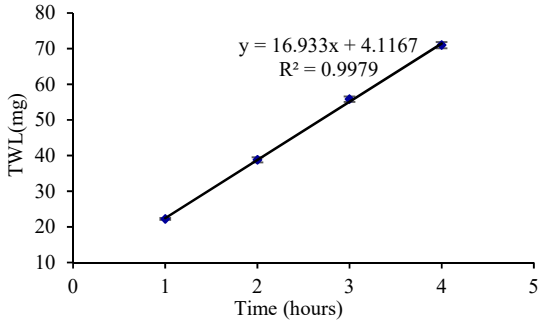

Fig. 3 TWL as a function of time at 29-33 °C, 20 m/s, and 600 mg/l solid loading in 3.5 % NaCl water

Fig. 5 shows the SEM image of a region of surface 2 mm away from the center, after 4-hour impingement, for a jet velocity of 20m/s and a sand concentration of 600 mg/l. Fig. 5 shows a significant amount of material loss. The impingement angle away from the specimen center is less than 90°, as shown in Fig. 6. This is consistent with the observations of Parsi et al. [17], that ductile materials have a higher erosion rate at lower impact angles caused by formation and cutting of platelets. The outer region in Fig. 7 (diameter (ø)>3 mm) shows aligned discrete cutting tracks and elongated pits in the direction of flow away from the center.

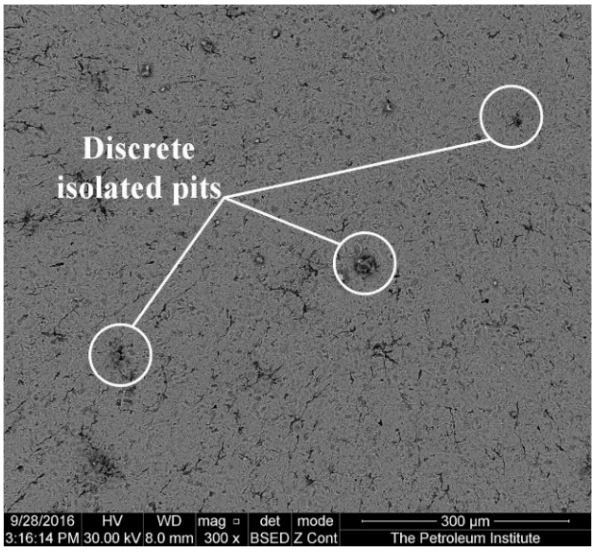

(a)

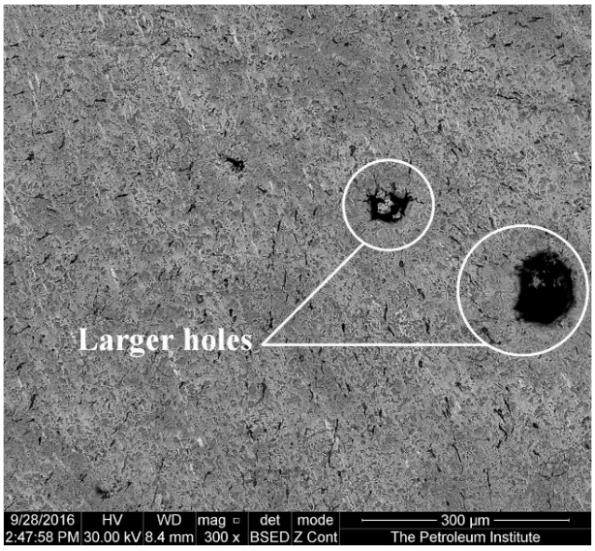

(b)

Fig. 4 SEM image center of the specimen after jet impingement test for erosion-corrosion study at 29-33 °C, 20m/s, 600 mg/l after (a) 1 hour (b) 4 hours

Figs. 8 and 9 show that the TWL varies linearly with both the jet velocity and the sand loading. It should be noted that the material removal increases at a much faster with the jet velocity than it does with the sand loading. The linear relationship between the TWL and sand loading was also obtained by others [4], [7], for different stainless steels.

The SEM image (Fig. 10) of the specimen under low impingement jet velocity (10 m/s) shows only a few pits beneath the impingement.

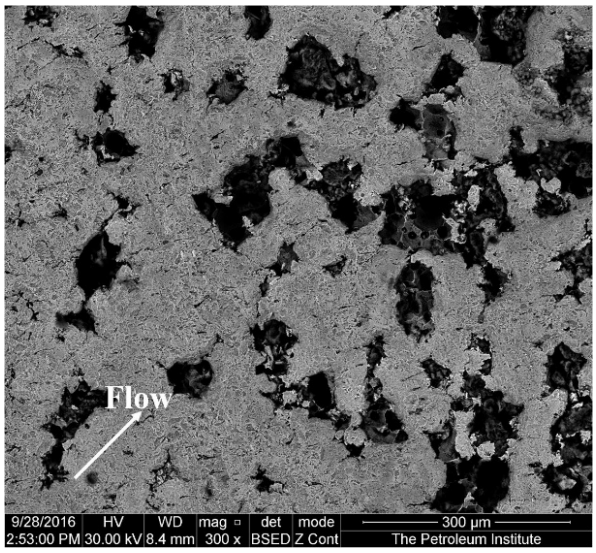

Fig. 5 SEM image of specimen 2 mm away from the center after jet impingement test for erosion-corrosion study at 29-33 °C, 20 m/s, 600mg/l, 4 hours

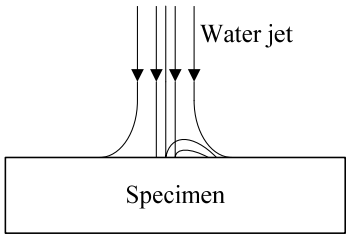

Fig. 6 Schematic of impingement of water jet on specimen surface

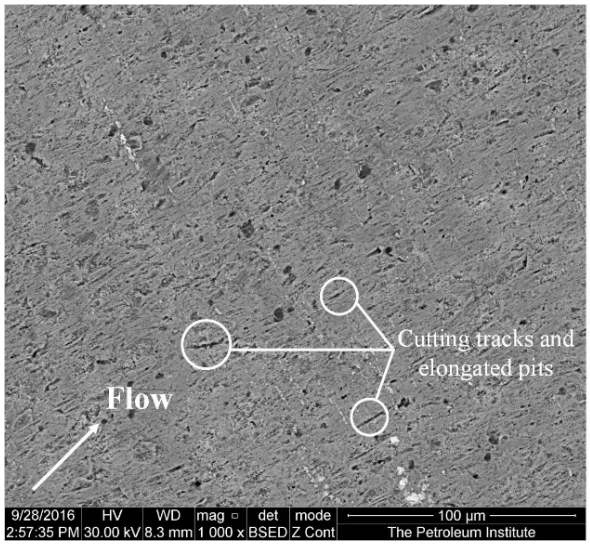

Fig. 7 SEM image of specimen under impinging jet, 3 mm away from center (at 29-33 °C, 20m/s, 600 mg/l, 4 hours

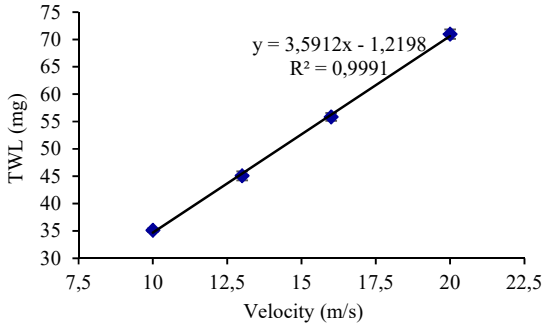

Fig. 8 TWL as a function of velocity at 29-33 °C and 600 mg/l solid loading in 3.5% NaCl water

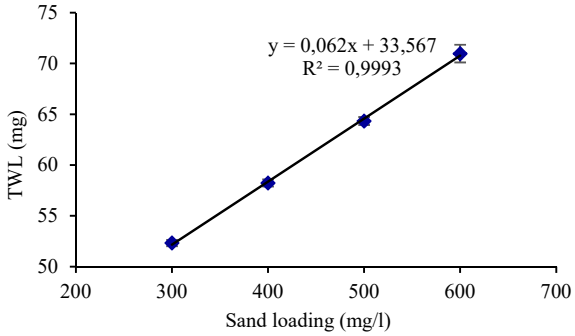

Fig. 9 TWL as a function of sand loading at 29-33 °C and 20 m/s in 3.5% NaCl water

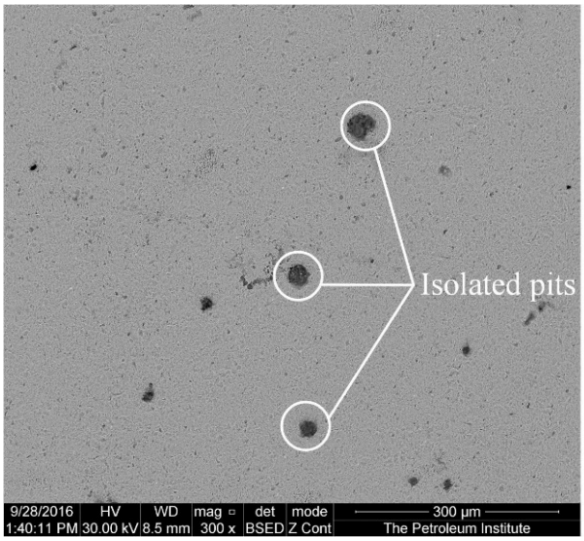

Fig. 10 SEM image center of the specimen after jet impingement test for erosion-corrosion study at 29-33 °C, 10 m/s, 600mg/l

B. Observations from Static Corrosion, Pure Erosion and Erosion-Corrosion Interactions

The effect of jet velocity and sand loading on weight loss due to pure erosion and erosion-corrosion interactions (E-C interaction, sum of synergistic and additive effects) are presented in Figs. 11 and 12. The E-C interaction is calculated by subtracting the pure erosion and static corrosion from the TWL. As it was the case for the TWL, the weight loss due to both pure erosion and E-C interaction increases linearly with

the jet velocity and the sand loading. The pure erosion is more dominant than E-C interaction for all velocities and sand loading considered as it contributes more weight loss to the TWL.

The SEM image of specimen 2 mm away from the center for pure erosion tests shows the formation of metal flakes on the surface due to impingement of particles (Fig. 13). These flakes indicate plastic deformation of the surface caused by multiple impacts. Fig. 5 shows the specimen surface, 2 mm away from the center after impingement under erosion-corrosion under the same conditions as in Fig. 13. The surface shows craters and an increase in material loss due to the combined effects of erosion and corrosion. These results are consistent with the platelet mechanism by Levy [18]. This leads to the conclusion that erosion is enhanced by corrosion, resulting in the detachment of flakes formed by multiple impacts of particles [19].

Fig. 14 shows the change in weight loss due to static corrosion with time. The contribution of pure corrosion to the TWL is insignificant, e.g. at 20 m/s, 600 mg/l after 4 hours of impingement, corrosion counts for only 0.59% of the TWL. Pure erosion seems to be the dominant factor as it contributes to more weight loss than static corrosion and E-C interaction.

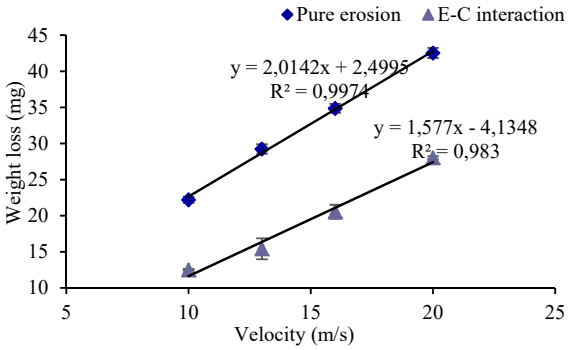

Fig. 11 Weight loss due as a function of velocity at 29-33 °C and 600 mg/l solid loading

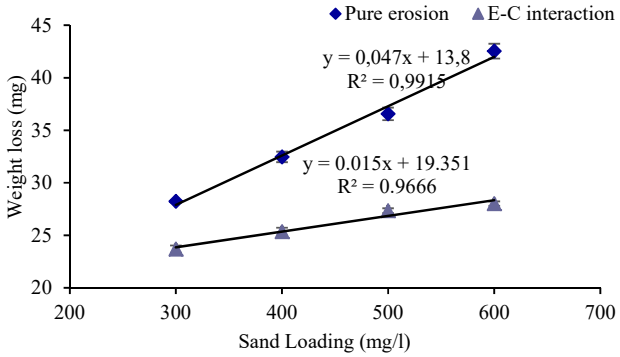

Fig.12 Weight loss as a function of sand loading at 29-33 °C and 20 m/s

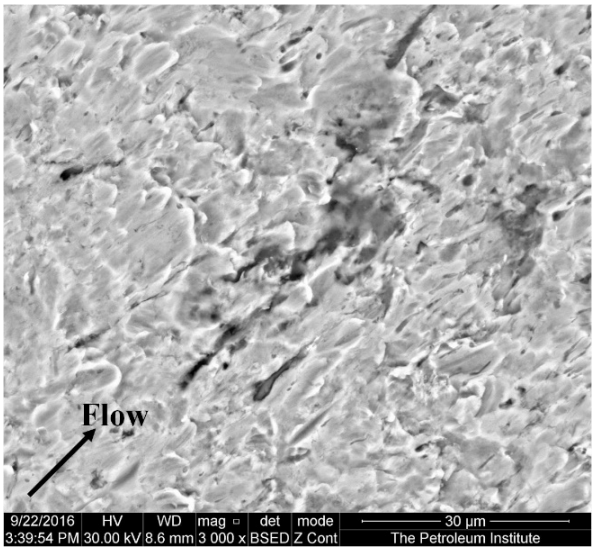

Fig. 13 SEM image of specimen 2 mm away from the center after jet impingement test for pure erosion study at 29-33 °C, 20m/s, 600mg/l, 4 hours

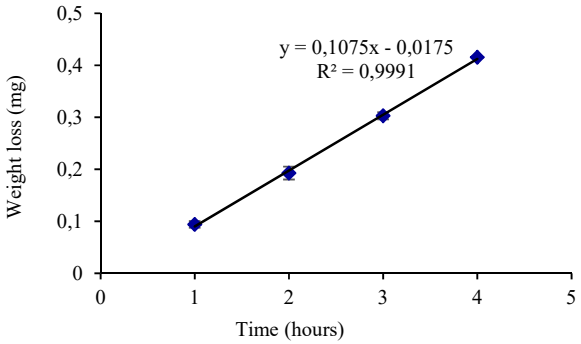

Fig. 14 Weight loss due to static corrosion as a function of time at 29-33 °C

IV. Conclusion

1. The contribution of weight loss due to static corrosion, pure erosion and erosion-corrosion interactions to the TWL was measured using a SIJ apparatus. The effects of velocity and sand loading on all the processes were analyzed.
2. The contribution of weight loss due to static corrosion is much less than the other processes involved.
3. Erosion is more dominant under all conditions.
4. The velocity and sand loading have a significant effect on TWL due to erosion-corrosion, pure erosion and erosion-corrosion interaction.

References

[1] H. Meng, X. Hu, and A. Neville, "A systematic erosion–corrosion study of two stainless steels in marine conditions via experimental design," *Wear,* vol. 263, pp. 355-362, 2007.

[2] F. Mohammadi and J. Luo, "Effects of particle angular velocity and friction force on erosion enhanced corrosion of 304 stainless steel," *Corrosion Science,* vol. 52, pp. 2994-3001, 2010.

[3] A. Neville, M. Reyes, and H. Xu, "Examining corrosion effects and corrosion/erosion interactions on metallic materials in aqueous slurries," *Tribology International,* vol. 35, pp. 643-650, 2002.
[4] X. Hu and A. Neville, "The electrochemical response of stainless steels in liquid–solid impingement," *Wear,* vol. 258, pp. 641-648, 2005.
[5] B. Jana and M. Stack, "Modelling impact angle effects on erosion–corrosion of pure metals: construction of materials performance maps," *Wear,* vol. 259, pp. 243-255, 2005.
[6] X. Hu and A. Neville, "CO 2 erosion–corrosion of pipeline steel (API X65) in oil and gas conditions—a systematic approach," *Wear,* vol. 267, pp. 2027-2032, 2009.
[7] X. Hu and A. Neville, "An examination of the electrochemical characteristics of two stainless steels (UNS S32654 and UNS S31603) under liquid–solid impingement," *Wear,* vol. 256, pp. 537-544, 2004.
[8] A. Neville and X. Hu, "Mechanical and electrochemical interactions during liquid–solid impingement on high-alloy stainless steels," *Wear,* vol. 251, pp. 1284-1294, 2001.
[9] X. Hu, R. Barker, A. Neville, and A. Gnanavelu, "Case study on erosion–corrosion degradation of pipework located on an offshore oil and gas facility," *Wear,* vol. 271, pp. 1295-1301, 2011.
[10] V. Souza and A. Neville, "Corrosion and synergy in a WC Co Cr HVOF thermal spray coating—understanding their role in erosion–corrosion degradation," *Wear,* vol. 259, pp. 171-180, 2005.
[11] A. Neville and T. Hodgkiess, "Characterisation of high-grade alloy behaviour in severe erosion–corrosion conditions," *Wear,* vol. 233, pp. 596-607, 1999.
[12] A. Neville, T. Hodgkiess, and J. Dallas, "A study of the erosion-corrosion behaviour of engineering steels for marine pumping applications," *Wear,* vol. 186, pp. 497-507, 1995.
[13] M. Naz, N. Ismail, S. Sulaiman, and S. Shukrullah, "Electrochemical and Dry Sand Impact Erosion Studies on Carbon Steel," *Scientific reports,* vol. 5, 2015.
[14] N. Smart, R. Bhardwaj, and J. O. M. Bockris, "Kinetic, solution, and interfacial aspects of iron corrosion in heavy brine solutions," *Corrosion,* vol. 48, pp. 764-779, 1992.
[15] J. Guiñón, J. García-Antón, V. Pérez-Herranz, and G. Lacoste, "Corrosion of carbon steels, stainless steels, and titanium in aqueous lithium bromide solution," *Corrosion,* vol. 50, pp. 240-246, 1994.
[16] A. N. S. Shrestha, T. Hodgkiess, "Electrochemical and mechanical during erosion–corrosion of high-velocity oxy-fuel (HVOF) coatings," *Wear,* vol. 235, pp. 623-634, 1999.
[17] M. Parsi, K. Najmi, F. Najafifard, S. Hassani, B. S. McLaury, and S. A. Shirazi, "A comprehensive review of solid particle erosion modeling for oil and gas wells and pipelines applications," *Journal of Natural Gas Science and Engineering,* vol. 21, pp. 850-873, 2014.
[18] A. V. Levy, *Solid particle erosion and erosion-corrosion of materials*: Asm International, 1995.
[19] R. Malka, S. Nešić, and D. A. Gulino, "Erosion–corrosion and synergistic effects in disturbed liquid-particle flow," Wear, vol. 262, pp. 791-799, 2007.